Fibrinogen-like globe domain of human Tenascin-C (hFBG-C)

A Target Enabling Package (TEP)

Gene ID / UniProt ID / EC	3371 / P24821 / -
Target Nominator	Kim S. Midwood[1]
Authors	Jesse A. Coker[1,2], Anna Marzeda[1], Anja Schwenzer[1], Brian D. Marsden[1,2], Kim S. Midwood[1], Wyatt W. Yue[2].
Therapeutic Area(s)	Inflammatory disease
Disease Relevance	FBG-C is an endogenous pro-inflammatory "damage-associated molecular pattern" that contributes to autoimmune disease like rheumatoid arthritis
Date Approved by TEP Evaluation Group	27th November 2020
Document version	1.0
Document version date	December 2020
Citation	Jesse A. Coker, Anna Marzeda, Anja Schwenzer, Brian D. Marsden, Kim S. Midwood, & Wyatt W. Yue. (2020). Fibrinogen-like globe domain of human Tenascin-C (hFBG-C); A Target Enabling Package [Data set]. Zenodo. http://doi.org/10.5281/zenodo.4429073
Affiliations	[1]Kennedy Institute of Rheumatology, University of Oxford, Nuffield Department of Orthopaedics, Rheumatology and Musculoskeletal Sciences, [2]Structural Genomics Consortium, University of Oxford, Nuffield Department of Medicine.

USEFUL LINKS

(Please note that the inclusion of links to external sites should not be taken as an endorsement of that site by the SGC in any way)

SUMMARY OF PROJECT

Chronic activation of the innate immune system by the damage-associated molecular pattern FBG-C (C-terminal fibrinogen-like globe domain of Tenascin-C) contributes to a variety of inflammatory diseases including arthritis, systemic sclerosis, and cancer. This TEP summarizes the first reported efforts to develop small-molecule FBG-C binders, with the aim to disrupt FBG-C-mediated pro-inflammatory protein-protein interactions (PPIs). We present the soluble expression of disulphide-containing human FBG-C (hFBG-C) in *E. coli*, the novel structure of hFBG-C, and preliminary chemical matter against hFBG-C derived from a crystallographic fragment screen. Finally, we introduce two robustly validated cellular assays, in either immortalized monocytes or primary human macrophages, which provide a route to development of small molecules which inhibit hFBG-C-activated inflammation.

SCIENTIFIC BACKGROUND

Tenascin-C (TN-C) is a large, hexameric, multi-domain extracellular matrix protein with restricted basal expression in adult tissues but that is transiently upregulated at sites of inflammation and/or tissue damage.[1]

TN-C participates in the global inflammatory response to tissue damage throughout the body, and during normal conditions contributes to promoting tissue repair.[2] However, unresolved TN-C expression leads to a chronic inflammatory state, which can spiral into *bona fide* autoimmune disease since TN-C activates its own expression.[3] TN-C is strongly upregulated in stroma from solid tumours, drives organ fibrosis in patients with system sclerosis, and is causative of arthritic joint disease.[4,5]

Many of the pathological consequences of TN-C are thought to stem from activation of the classic innate immune receptor toll-like receptor 4 (TLR4), which canonically activates inflammation in response to bacterial endotoxin (LPS).[6] However, recent evidence shows that TN-C is one of dozens of endogenous damage-associated molecular patterns (DAMPs) which activate inflammation via TLRs in the absence of infection.[7] The human *TNC* contains 30 exons which are often alternatively spliced; however, the most important domain in the context of chronic inflammation and the focus of this TEP is the 27 kDa disulphide-stabilized C-terminal fibrinogen-like globe domain (hFBG-C), which was conclusively mapped as the TLR4-activating region of TN-C.[8] hFBG-C belongs to a family of 21 human proteins known as the fibrinogen related protein (FRePs), which carry out diverse signalling roles and engage different receptors, but all share a conserved FBG domain.[9] Inhibiting pro-inflammatory TLR4 signalling activated by hFBG-C represents an underexplored therapeutic hypothesis, and insights gleaned from targeting hFBG-C could provide strategic insight into inhibiting the action of other disease relevant FRePs.

A start-up biotech company, Nascient Ltd., has developed high affinity neutralizing anti-FBG-C monoclonal antibodies which show promise in animal models of RA and are moving into preliminary clinical trials.[10] However, accumulating evidence points strongly to a TLR4-containing cell-surface complex composed of many proteins that assemble and differentially interact to tune pro-inflammatory signalling in response to FBG-C.[11,12] Furthermore, FBG-C is known to bind to other cell-surface receptors using distinct epitopes from the TLR4-binding region.[13] Therefore, unlike a monoclonal antibody, which will broadly neutralize all FBG-C mediated PPI's due to the small size of FBG-C (27 kDa), a small molecule inhibitor could selectively inhibit only a subset of FBG-C-mediated PPIs. These data provide a rationale for the development of interaction-specific inhibitors that could perhaps pave the way for targeted therapies, especially as details surrounding the innate immune recognition of endogenous DAMPs emerge in the future.

RESULTS – THE TEP

Proteins Purified

hFBG-C is a compact, disulphide-stabilized 27 kDa domain with no predicted active sites or druggable pockets. Improving upon a tedious and refolding methodology previously reported in literature, we optimized the soluble expression and purification of hFBG-C from disulphide-refolding "CyDisCo" *E. coli* cell lines.[14] Our method takes just 36 hours from lysis to freezer, whilst the previous refolding methodology requires up to ten full days. We purified both full-length hFBG-C (I1974—A2201) and a truncated crystallisable construct (P1979—G2196), which we express using a His- or His-Twin-Strep tag™ with or without a C-terminal biotinylation peptide (**Fig 1a**). All four recombinant proteins are pure (**Fig 1b**), monodisperse (**Fig 1d**), and contain the expected two intramolecular disulphide bonds (**Fig 1c**). Using DSF, we also demonstrated that hFBG-C binds Ca^{2+}, likely at the known "DXD" cation binding loop (**Fig 1e**), albeit more weakly than other FRePs from the angiopoietin-like protein family (AGL1, 2, and 6).

Structural Data

We determined the novel 1.4 Å resolution crystal structure of hFBG-C (PDB: 6QNV) using the construct hFBG-C ΔCTL. The fold of hFBG-C matches the classic three-subdomain "ABP" architecture associated with the FRePs (**Fig 2a**), with a 7-strand β-sheet providing the backbone to support a variable, loop-filled P-subdomain.[15] In agreement with bioinformatic predictions, hFBG-C contains no active sites or obvious hydrophobic pockets, but the structure does allow us to visualize the known TLR4-binding "cationic ridge" (**Fig 2a, 2b**), which was recently mapped by Zuliani-Alvarez *et al*.[8] Consistent with the notion of this cationic ridge as a PPI-mediator, the key stretch of basic residues is solvent exposed and protrudes outward from the core of the domain (see

Fig 2a, surface view). In other FReP structures [including two determined in our group, namely ANGPTL2 (PDB: 6Y41) and ANGPTL6 (PDB: 6Y43)], the disordered segment of so-called "peptide 7" (light green, **Fig 2a**) is ordered and bound to Ca^{2+} by the corresponding DXD motif. Therefore, our structure demonstrates that the calcium-binding loop of hFBG-C is highly flexible in the absence of Ca^{2+}. hFBG-C crystallizes as a monomer, consistent with all of our solution state data (**Fig 1d**).

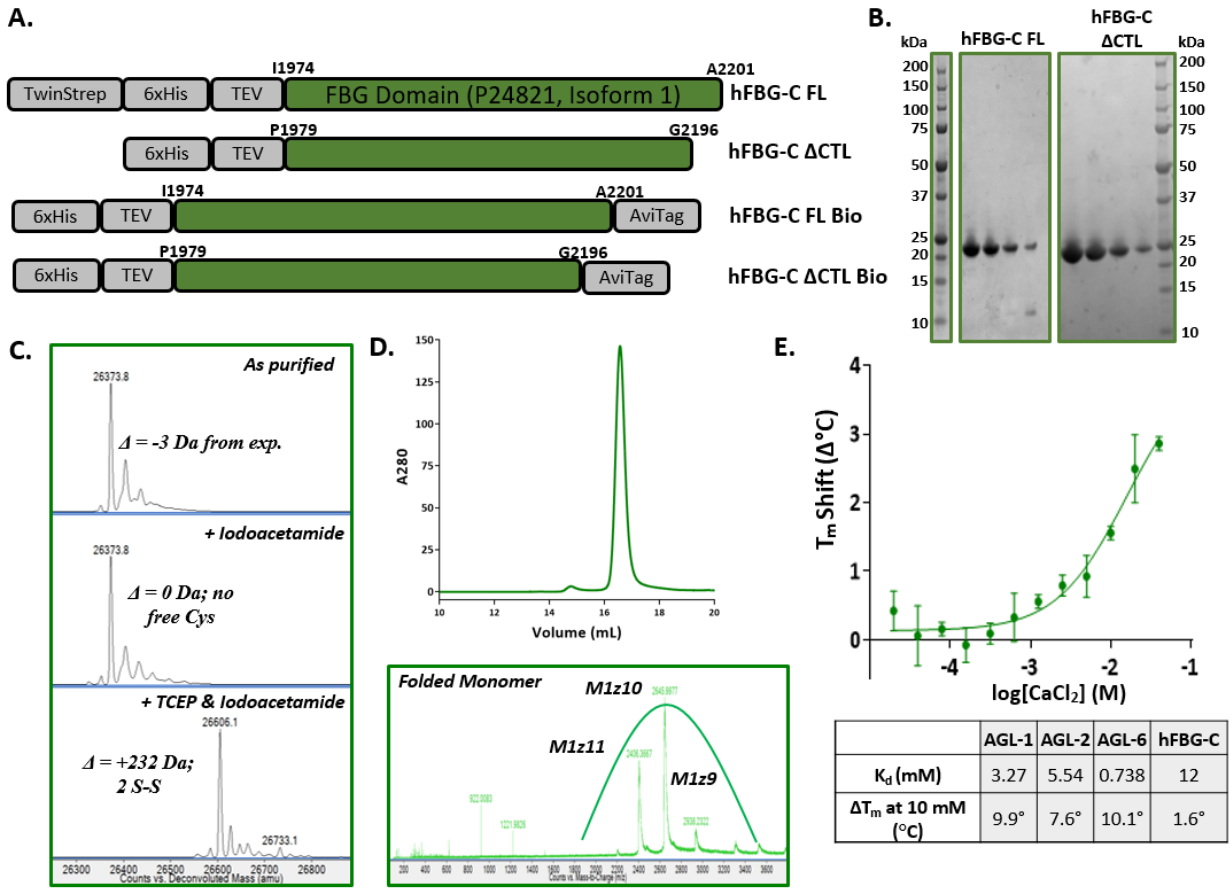

	AGL-1	AGL-2	AGL-6	hFBG-C
K_d (mM)	3.27	5.54	0.738	12
ΔT_m at 10 mM (°C)	9.9°	7.6°	10.1°	1.6°

Figure 1 (A) hFBG-C construct design for E. coli expression. (B) Representative final purity for hFBG-C proteins. (C) Intact mass analysis shows the proper formation of two disulphide bonds. (D) hFBG-C is a monodisperse monomer, confirmed by analytical size-exclusion chromatography (top) and Native-MS (bottom). (E) hFBG-C binds to Ca^{2+} in a thermal shift DSF assay, but more weakly than other homologues with a similar cation binding motif (AGL1, AGL2, and AGL6).

Fragment Screen and Chemical Matter

After optimizing the crystal system which led to the novel hFBG-C structure, we conducted an XChem fragment screening campaign at Diamond Light Source. After soaking 330 hFBG-C crystals, we collected 300 datasets with an average resolution of 1.7 Å. After manually evaluating the 68 interesting densities identified by the PanDDA software, we found eleven fragment hits across three different sites (**Fig 2b**). Interestingly, despite no obvious hydrophobic pockets in our original structure, we identified a fragment binding hotspot (Site 1) on the reverse face of the protein from the TLR4 binding epitope which appears upon displacement of R2050. This pocket binds 8 different fragments and accommodates predominately *para*-substituted phenyl rings, with electron-rich groups including halogens (fragments 2, 3, and 6) and nitriles (fragments 5, 7, and 8) seeming particularly preferred. We also identified two adjacent fragments, 10 and 11, both binding near the TLR4 binding ridge in a shelf formed by part of the core beta-sheet within the B-subdomain. Despite its shallow, surface exposed nature, residues in the "beta shelf" participate in two (fragment 11) or three (fragment 10) hydrogen bonds, suggesting reasonable affinity could be engineered at Site 3 (**Fig 2b**). Finally, one hit (fragment 9) binds to Site 2, which comprises a narrow cleft formed next to Phe2191 and directly above Site 3; this site is distal from the TLR4-binding region and is not stabilized by hydrogen bonds, making it the least

promising of the three sites. Given the lack of known active sites or deep hydrophobic pockets on hFBG-C, our fragment screen provides an unprecedented starting point for the development of PPI inhibitors targeting two faces of the hFBG-C domain. A table of fragment-by-fragment binding details, including fragment identifiers and PDB ID's, is provided in the Additional Information below.

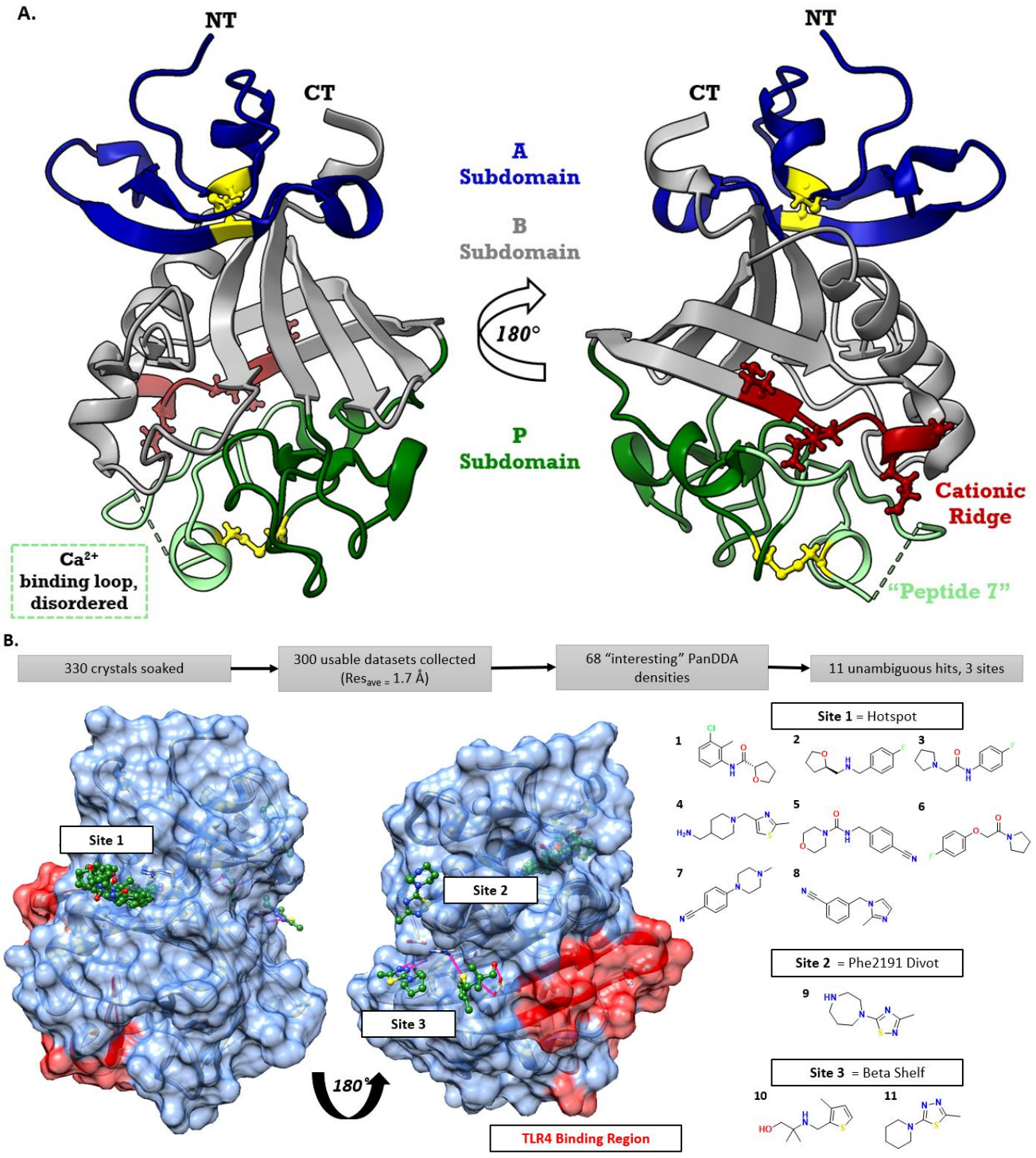

Figure 2 (A) Novel structure of hFBG-C reveals the architecture of the domain along with the location of the TLR4 binding site, known as the cationic ridge (red). Disulphide bonds in yellow ball and stick representation, partially disordered Ca^{2+}-binding "peptide 7" highlighted in light green. **(B)** Crystallographic fragment screen reveals 11 fragment hits across 3 distinct sites, including the hotspot Site 1 and the TLR4-binding-region-adjacent Site 3. Hydrogen bonds at Site 3 are displayed in pink.

Assays

To further characterize pro-inflammatory signalling in response to recombinant hFBG-C, we developed two cellular assays which measure transcriptional and protein-level responses upon stimulation with endotoxin-free (<10 pg/mL) hFBG-C FL. **Fig 3a** highlights a small titration of hFBG-C in our NF-κB reporter assay in immortalized THP1-Blue™ monocytes. Activation of NF-κB leads to transcription and secretion of alkaline phosphatase, which can be easily qualified colorimetrically.[16] Notably, even 0.5 µM hFBG-C activates NF-κB, whilst 5.0 µM hFBG-C stimulates as robust a pro-inflammatory response as the classic innate immune activator, LPS. Secondly, in an effort to create a more biologically relevant system, we implemented a 96-well ELISA using primary human macrophages (**Fig 3b**)**.** Stimulation of primary human macrophages with increasing doses of hFBG-C leads to robust and dose-dependent induction of the pro-inflammatory cytokines TNFα, IL6, and IL-8. As in the NF-κB assay, moderate concentrations of hFBG-C (2 µM or less) are often even stronger agonists than LPS. Importantly, induction of pro-inflammatory cytokines is reversed by treatment with either TAK242 (a small molecule TLR4 inhibitor that binds to the cytosolic portion of the receptor) or with a poly-clonal anti-TLR4 antibody (**Fig 3c**), validating that hFBG-C potently activates macrophages via its known receptor TLR4.[17] Both of these assays work in a 96-well format, and we expect the NF-κB report assay to be amenable to miniaturization into 384-well formats. Therefore, these assays provide a simple, reliable, and phenotypic system for characterizing small-molecule inhibitors of hFBG-C-stimulated inflammation.

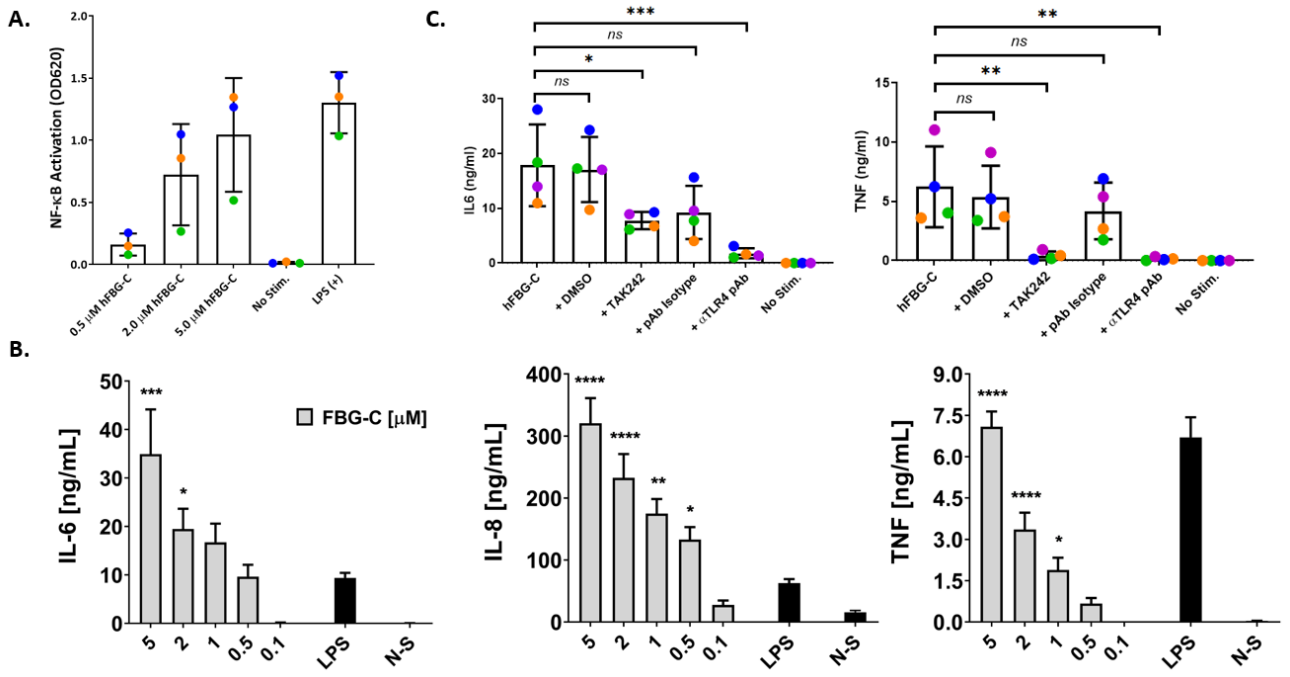

Figure 3 (A) hFBG-C activation of NF-κB signalling using immortalized THP1-Blue™ monocytes is concentration-dependent and similar in magnitude to LPS activation (n = 3; mean ± SD, individual replicates coloured distinctly). (B) Primary human macrophages were stimulated with decreasing concentrations of hFBG-C, LPS (EH100) at 1 ng/mL, or were left unstimulated (N-S) for 24h, and IL-6, IL-8 and TNF levels were measured by ELISA. Data are shown as mean ± SEM from 4 independent donors. Data was analysed using a one-way ANOVA vs non-stimulated, *p<0.05, **p<0.01, ***p<0.001, ****p<0.0001. (C) Stimulation of primary human macrophages with 1 µM hFBG-C leads to the release of TNF and IL6 (n = 4; mean ± SD, individual donors coloured distinctly). The phenotype can be reversed with either a TLR4 inhibitor (TAK242) or a poly-clonal anti-TLR4 antibody (αTLR4 pAb), but not with DMSO or an isotype control. Means from four biological replicates were compared using an ordinary one-way ANOVA followed by Dunnett's test, *p<0.05, **p<0.01, ***p< 0.001.

Future Plans and Collaborations

This TEP contains data generated during an ongoing collaboration with the Midwood Lab at the Kennedy Institute, with the goal to understand the molecular details of FBG-C-activated TLR4 and leverage this knowledge for drug discovery. Data herein are included in two manuscripts under preparation, and we are actively using our optimized methodologies to interrogate the activity of the entire FReP family using cellular assays, proteomics, and orthogonal biophysical methods.

CONCLUSION

Herein, we present our efforts to develop small-molecule inhibitors targeting hFBG-C, including a novel structure of hFBG-C and a crystallographic fragment screen which identified eleven hFBG-C binders. This is the first ever report of chemical matter targeting hFBG-C, due in no small part to the discovery of a cryptic fragment-binding hotspot. The screen also uncovered a shallow, surface-exposed, hydrogen-bond-driven binding site near the known TLR4-binding cationic ridge which, although likely challenging to ligand with a small molecule, provides a mapped target site for other therapeutic modalities like biologics or cyclic peptides. We also present multiple cell-based assays, including an ELISA in disease-relevant primary human macrophages and an NF-κB reporter system in immortalized monocytes, which can be used in the future to develop and characterize small molecules which inhibit hFBG-C-activated transcriptional responses and cytokine release. Finally, because hFBG-C participates in a diverse network of PPI's, our fragment hits could provide starting points for developing targeted PPI inhibitors that disrupt only pathogenic PPI's and perhaps outperform the fully neutralizing monoclonal antibodies already in pre-clinical development.

FUNDING INFORMATION

The work performed at the SGC has been funded by a grant from the Wellcome [106169/ZZ14/Z]. J.A.C is a DPhil candidate fully supported by the Nuffield Department of Medicine's Prize Studentship.

ADDITIONAL INFORMATION

Structure Files

PDB ID	Structure Details
6QNV	Novel structure of hFBG-C
5R5T – 5R63	Group deposition of 11 fragment bound hFBG-C structures

Fragment-by-Fragment Details

Fragments are coloured by heteroatom with dark green carbons. Residues in contact with the fragments are coloured by heteroatom (nitrogen blue, oxygen red) while the hFBG-C backbone and surface is coloured grey.

PDB	Unique Identifiers	Fragment Structure	Binding Location	Binding Pocket	Resolution (Å)
5R5U	*xtal:* x0084 *fragment:* Z1545312521	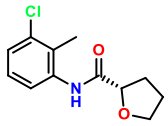	Site 1 Hotspot	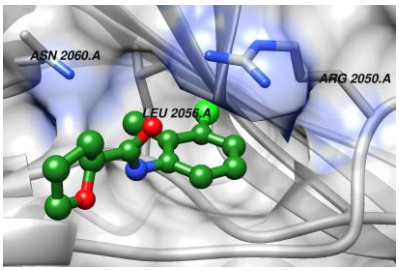	1.52
5R5V	*xtal:* x0141 *fragment:* Z2856434824	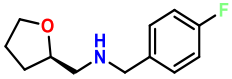	Site 1 Hotspot	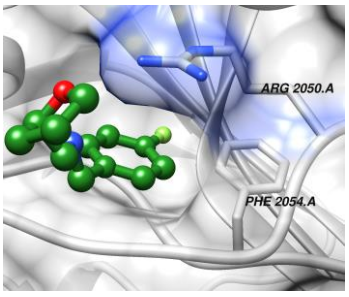	1.70
5R5W	*xtal:* x0162 *fragment:* Z2856434942	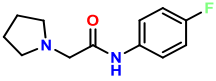	Site 1 Hotspot	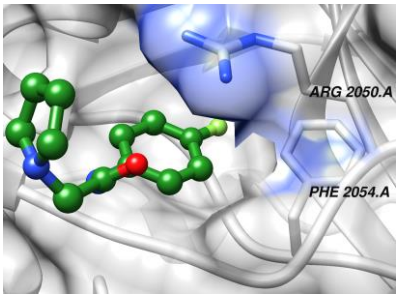	1.60
5R5X	*xtal:* x0179 *fragment:* Z1259335913	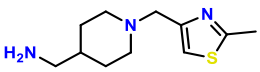	Site 1 Hotspot	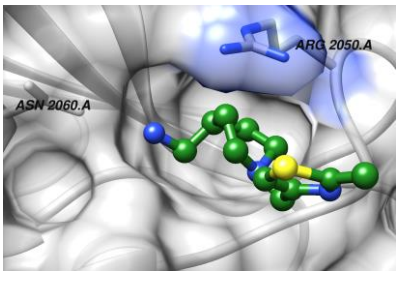	1.56

5R5Y	*xtal:* x0192 *fragment:* Z509756472	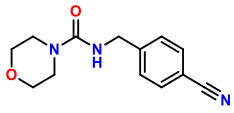	Site 1 Hotspot	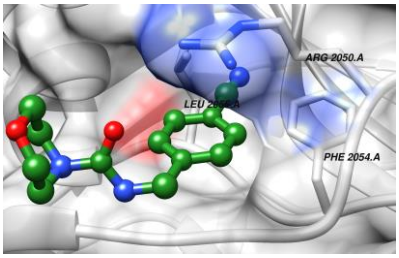	1.57
5R60	*xtal:* x0245 *fragment:* Z19735067	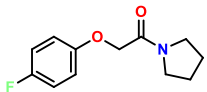	Site 1 Hotspot	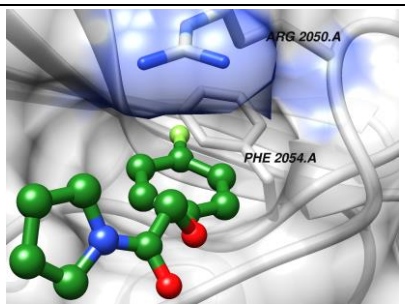	1.79
5R62	*xtal:* x0291 *fragment:* Z2856434840	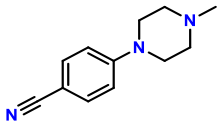	Site 1 Hotspot	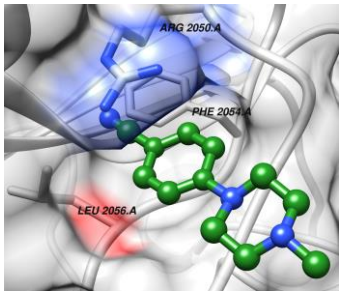	1.40
5R63	*xtal:* x0323 *fragment:* Z319545618	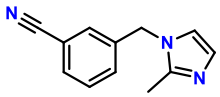	Site 1 Hotspot	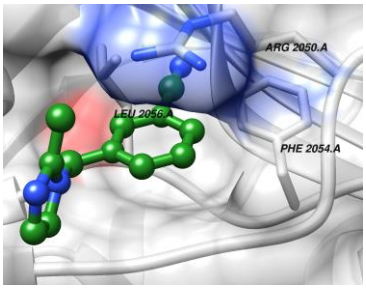	1.59
5R61	*xtal:* x0290 *fragment:* Z1578665941	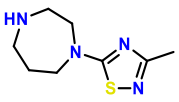	Site 2 Phe2191 Divot	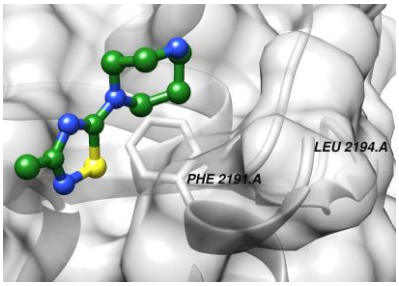	1.38
5R5Z	*xtal:* x0228 *fragment:* Z2856434821	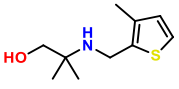	Site 3 Beta Shelf	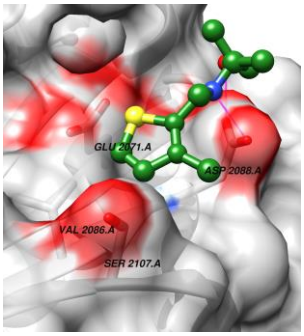	1.67

5R5T	*xtal:* x0063 *fragment:* Z1251207602	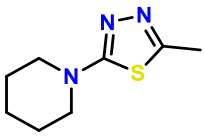	Site 3 Beta Shelf	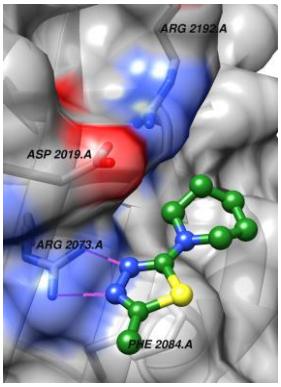	1.55

Materials and Methods

Protein Expression and Purification

Construct Details

hFBG-C FL (TNCA-c025):

Ile1974—Ala2201 + N-terminal, TEV-cleavable hexahistidine Twin-strep-tag®

hFBG-C ΔCTL (TNCA-c042):

Pro1979—Gly2196 + N-terminal, TEV-cleavable hexahistidine tag

hFBG-C FL Bio (TNCA-c049):

Ile1974—Ala2201 + N-terminal, TEV-cleavable hexahistidine tag + C-terminal AviTag™

hFBG-C ΔCTL Bio (TNCA-c050):

Pro1979—Gly2196 + N-terminal, TEV-cleavable hexahistidine tag + C-terminal AviTag™)

Accession: P24821 Isoform 1 (NM_002160.3) + Natural Variant E2008Q.
Expression Cell Line: BL21(DE3) Tuner + CyDisCo pMJS226
Vectors Used: pNIC-NHStIIT**,** pNIC28-Bsa4, or pNIC-Bio3

Sequence Details

Bold = tag sequence
Bold + Italics = removed by TEV protease
Underlined = hFBG-C

>TNCA-c025 (hFBG-C FL)

***MHHHHHHSSGASWSHPQFEKGGGSGGGSGGSAWSHPQFEKGSGVDLGTENLYFQ*SM**IGLLYPFPKDCSQA
MLNGDTTSGLYTIYLNGDKAQALEVFCDMTSDGGGWIVFLRRKNGRENFYQNWKAYAAGFGDRREEFWLGLD
NLNKITAQGQYELRVDLRDHGETAFAVYDKFSVGDAKTRYKLKVEGYSGTAGDSMAYHNGRSFSTFDKDTDSAIT
NCALSYKGAFWYRNCHRVNLMGRYGDNNHSQGVNWFHWKGHEHSIQFAEMKLRPSNFRNLEGRRKRA

>TNCA-c042 (hFBG-C ΔCTL)

***MHHHHHHSSGVDLGTENLYFQ*SM**PFPKDCSQAMLNGDTTSGLYTIYLNGDKAQALEVFCDMTSDGGGWIVFL
RRKNGRENFYQNWKAYAAGFGDRREEFWLGLDNLNKITAQGQYELRVDLRDHGETAFAVYDKFSVGDAKTRYK

LKVEGYSGTAGDSMAYHNGRSFSTFDKDTDSAITNCALSYKGAFWYRNCHRVNLMGRYGDNNHSQGVNWFH
WKGHEHSIQFAEMKLRPSNFRNLEG

>TNCA-c049 (hFBG-C FL Bio)
MHHHHHHSSGVDLGTENLYFQ**SM**IGLLYPFPKDCSQAMLNGDTTSGLYTIYLNGDKAQALEVFCDMTSDGGG
WIVFLRRKNGRENFYQNWKAYAAGFGDRREEFWLGLDNLNKITAQGQYELRVDLRDHGETAFAVYDKFSVGDA
KTRYKLKVEGYSGTAGDSMAYHNGRSFSTFDKDTDSAITNCALSYKGAFWYRNCHRVNLMGRYGDNNHSQGV
NWFHWKGHEHSIQFAEMKLRPSNFRNLEGRRKRA**SSKGGYGLNDIFEAQKIEWHE**

>TNCA-c050 (hFBG-C ΔCTL Bio)
MHHHHHHSSGVDLGTENLYFQ**SM**PFPKDCSQAMLNGDTTSGLYTIYLNGDKAQALEVFCDMTSDGGGWIVFL
RRKNGRENFYQNWKAYAAGFGDRREEFWLGLDNLNKITAQGQYELRVDLRDHGETAFAVYDKFSVGDAKTRYK
LKVEGYSGTAGDSMAYHNGRSFSTFDKDTDSAITNCALSYKGAFWYRNCHRVNLMGRYGDNNHSQGVNWFH
WKGHEHSIQFAEMKLRPSNFRNLEG**SSKGGYGLNDIFEAQKIEWHE**

Protein Expression and Purification Method
hFBG-C constructs were transformed by heat shock into chemically competent BL21(DE3) Tuner *E. coli* cells, carrying the ChlorR CyDisCo helper plasmid pMJS226 which was a gift from Prof. Lloyd Ruddock and allows the soluble over-expression of disulphide-containing proteins in the cytoplasm.[14] Overnight cultures were inoculated 1:100 into "TB-PLUS" media (1X Terrific Broth + 15 mL/L glycerol + 0.01% Antifoam + 1 mM $MgSO_4$ + 10 mM $(NH_4)_2SO_4$ + 0.5% (w/v) glucose + 1X E. coli trace metals) and grown at 30°C with 250 RPM shaking to OD = 2.5. Expression was induced with 0.5 mM IPTG and allowed to proceed overnight at 18°C. For biotinylated constructs (TNCA-c049 and -c050), 1 g/L of D-biotin (Fluorochem) was added at time of induction. Cells were harvested by centrifugation, lysed by sonication in Lysis Buffer 1 or Lysis Buffer 2 (biotinylated constructs), and clarified by centrifugation (> 15,000 x *g,* 60 min). For the first affinity step, either TALON® Superflow™ (TNCA-c042, -c049, -c050) or StrepTactinXT™ (TNCA-c025) resin was used essentially according to the manufacturer's recommendations, and hFBG-C was eluted with Elution Buffer 1 (TALON®) or Elution Buffer 2 (StrepTactinXT™). N-terminal tags were removed via TEV cleavage (either 4 hours at room temperature or overnight at 4°C) and the cleavage efficiency (100%), biotinylation efficiency (>99%), and intact mass were confirmed by LC-MS according to standard methods.[18] Finally, the protein was polished on a Superdex 75 16/60 column into Gel Filtration Buffer, and the monodisperse, monomeric peak was concentrated to up to 30 mg/mL before flash freezing in LN_2 and storage at -80 °C.

a) Lysis Buffer 1: 50 mM HEPES pH = 7.5, 300 mM NaCl, 5% glycerol, 1X benzonase, 1X protease inhibitors
b) Lysis Buffer 2: 50 mM HEPES pH = 7.5, 300 mM NaCl, 5% glycerol, 1X benzonase, 1X protease inhibitors, 4 mM D-biotin
c) Elution Buffer 1: 50 mM HEPES pH = 7.5, 300 mM NaCl, 5% glycerol, 150 mM imidazole
d) Elution Buffer 2: 50 mM HEPES pH = 7.5, 300 mM NaCl, 5% glycerol, 50 mM D-biotin
e) Gel Filtration Buffer: 20 mM HEPES pH = 7.5, 250 mM NaCl, 2% glycerol

Disulphide Bond Validation by Intact Mass Spectrometry
To verify the presence of two disulphide bonds in purified hFBG-C, three samples were prepared for intact mass analysis. The first "as purified" Sample A was prepared and analysed as above. The second "+ iodoacetamide" Sample 2 was prepared by denaturing 5 µg of protein for 1 hour in 50 µL of Denaturing Buffer (8M Urea in 50 mM Ammonium Bicarbonate pH = 8.0), followed by the addition of 25 mM Iodoacetamide and a second 1 hour incubation prior to intact mass analysis. The third "+TCEP iodoacetamide" Sample 3 was prepared as for sample 2, except 10 mM TCEP was added to the Denaturing Buffer to reduce disulphide bonds prior to alkylation with iodoacetamide. Each alkylation event corresponds to a mass shift of 57-58 Da,

representing the capping of a single Cys residue. In protein with 2 properly formed disulphide bonds, an approximately 230 Da mass shift occurs in Sample 3 while no mass shift occurs in Sample 2 (all relative to as purified sample 1). hFBG-C preps were only used if the expected two disulphide bonds were observed.

Differential Scanning Fluorimetry for Calcium Binding

hFBG-C is known to bind Ca^{2+} at a mapped "DXD" cation binding loop (D2128—D2130). To validate this activity, we implemented a simple DSF assay essentially as described previously.[19] An 11-point serial dilution of $CaCl_2$ was prepared in water at 10X the desired final concentration. In a 96-well v-bottom white qPCR plate, 10 µL of 2X HEPES-buffer saline (HBS) was mixed with 4 µL of water, 2 µL of the 10X $CaCl_2$ dilution series, and 2 µL of protein at a stock concentration of 3 mg/mL (final concentration 0.3 mg/mL). Samples were incubated for 15 min at room temperature before the addition of 2 µL of 10X SYPRO™ Orange and a second 10 min incubation in the dark. Melt curves were collected on an MX3005p RT-PCR Machine (Stratagene) from 25°C to 95°C with a ramp of 1°C/min. Melt temperatures were calculated by nonlinear fitting to the ideal monophasic ProteoPlex model,[20] and K_d's were extracted by plotting T_m shifts (relative to protein in the absence of Ca^{2+}) against log[Ca^{2+}] and fitting to a one-site saturation binding model in GraphPad Prism.

Crystallization and Fragment Screening

Throughout, sitting-drop vapour diffusion experiments were performed in 96-well, three-sub-well SWISSCI plates. The structure of hFBG-C (PDB: 6QNV) was solved using a crystal which appeared after 28 days at 20°C with hFBG-C ΔCTL at 17 mg/mL mixed with Morpheus Condition C09 (0.09M NPS + 0.1M Buffer System 3 pH = 8.5 + 50% Precipitant Mix 1).[21] Crystals were flash frozen in LN_2 and data was collected at Diamond Light Source and automatically indexed, integrated, and scaled using the Xia2 pipeline.[22] The structure was phased by molecular replacement using Phaser (search model PDB: 1FIC),[23] followed by manual re-building in Coot and refinement in *phenix.refine*.[24,25]

For fragment screening, hFBG-C ΔCTL was concentrated to 30 mg/mL and mixed 100 nL : 100nL in all sub-wells of a SWISSCI plate using the custom fine screen "JAC-MorpheusC09-z001", which samples the chemical space around Morpheus C09 by varying the pH of Buffer System 3 from 7.0-9.0 and the concentration of Precipitant Mix 1 from 44% to 56%. After 14 days, > 150 crystals per plate were obtained and used to complete a full fragment screen of the DSI-Poised 1 Fragment Library (Enamine) at the XChem Facility, Diamond Light Source Beamline i04-1 according to standard methodologies (https://www.diamond.ac.uk/Instruments/Mx/Fragment-Screening.html). Followed by automatic data collection, data were imported to XChemExplorer,[26] phased by molecular replacement using Dimple,[27] and putative fragment binding events were identified by PanDDA.[28] Structures were manually triaged and 11 conclusively bound co-crystal structures were refined with REFMAC before deposition.[29]

Assays

Previously published, detailed step-by-step methods for the NF-κB reporter assay in THP1 Blue™ monocytes and the ELISA in primary human macrophages were followed as recommended.[16,17] Anti-TLR4 polyclonal antibody and isotype control were obtained from InvivoGen (PAb-hTLR4; https://www.invivogen.com/pab-htlr4). The final concentration of LPS in the cellular assays was strictly regulated to be < 10 pg/mL to avoid LPS-induced pro-inflammatory signalling. For hFBG-C FL expressed as a soluble protein as reported above, the final purified protein was concentrated to 30 mg/mL and LPS was removed with Thermo Scientific High Capacity Endotoxin Removal Resin according to the manufacturer's recommendations. Alternatively, endotoxin-free hFBG-C can be prepared by intentional formation of inclusion bodies via expression in standard BL21(DE3) *E. coli* cell lines, followed by purification, endotoxin removal, and refolding according to previously reported methodologies.[8] While we routinely obtain endotoxin-free hFBG-C using our method for use at 2 µM or below, care must be taken to ensure that the requisite LPS threshold is strictly maintained for the specific application and final assay concentration.

References

1. Midwood, K. S., Chiquet, M., Tucker, R. P. & Orend, G. Tenascin-C at a glance. *J. Cell Sci.* **129**, 4321–4327 (2016).
2. Midwood, K. S. & Orend, G. The role of tenascin-C in tissue injury and tumorigenesis. *J. Cell Commun. Signal.* **3**, 287–310 (2009).
3. Goh, F. G., Piccinini, A. M., Krausgruber, T., Udalova, I. A. & Midwood, K. S. Transcriptional Regulation of the Endogenous Danger Signal Tenascin-C: A Novel Autocrine Loop in Inflammation. *J. Immunol.* **184**, 2655–2662 (2010).
4. Bhattacharyya, S. *et al.* TLR4-dependent fibroblast activation drives persistent organ fibrosis in skin and lung. *JCI Insight* **3**, e98850 (2018).
5. Midwood, K. *et al.* Tenascin-C is an endogenous activator of Toll-like receptor 4 that is essential for maintaining inflammation in arthritic joint disease. *Nat. Med.* **15**, 774–780 (2009).
6. O'Neill, L. A. J., Golenbock, D. & Bowie, A. G. The history of Toll-like receptors — redefining innate immunity. *Nat. Rev. Immunol.* **13**, 453–460 (2013).
7. Midwood, K. S. & Piccinini, A. M. DAMPening inflammation by modulating TLR signalling. *Mediators Inflamm.* **2010**, (2010).
8. Zuliani-Alvarez, L. *et al.* Mapping tenascin-C interaction with toll-like receptor 4 reveals a new subset of endogenous inflammatory triggers. *Nat. Commun.* **8**, (2017).
9. Zuliani-Alvarez, L. & Midwood, K. S. Fibrinogen-Related Proteins in Tissue Repair: How a Unique Domain with a Common Structure Controls Diverse Aspects of Wound Healing. *Adv. Wound Care* **4**, 273–285 (2015).
10. Aungier, S. R. *et al.* Targeting early changes in the synovial microenvironment: A new class of immunomodulatory therapy? *Ann. Rheum. Dis.* **78**, 186–191 (2019).
11. Płóciennikowska, A., Hromada-Judycka, A., Borzęcka, K. & Kwiatkowska, K. Co-operation of TLR4 and raft proteins in LPS-induced pro-inflammatory signaling. *Cell. Mol. Life Sci.* **72**, 557–581 (2015).
12. Piccinini, A. M., Zuliani-Alvarez, L., Lim, J. M. P. & Midwood, K. S. Distinct microenvironmental cues stimulate divergent TLR4-mediated signaling pathways in macrophages. *Sci. Signal.* **9**, (2016).
13. Tucker, R. P. & Chiquet-Ehrismann, R. Tenascin-C: Its functions as an integrin ligand. *Int. J. Biochem. Cell Biol.* **65**, 165–168 (2015).
14. Gaciarz, A. *et al.* Efficient soluble expression of disulfide bonded proteins in the cytoplasm of Escherichia coli in fed-batch fermentations on chemically defined minimal media. *Microb. Cell Fact.* **16**, 1–12 (2017).
15. Yee, V. C. *et al.* Crystal structure of a 30 kDA C-terminal fragment from the γ chain of human fibrinogen. *Structure* **5**, 125–138 (1997).
16. Zuliani-Alvarez, L., Piccinini, A. & Midwood, K. Screening for Novel Endogenous Inflammatory Stimuli Using the Secreted Embryonic Alkaline Phosphatase NF-κB Reporter Assay. *Bio-Protocol* **7**, 1–12 (2017).
17. Murdamoothoo, D. *et al.* Investigating cell-type specific functions of tenascin-C. in *Methods Cell Biol* 401–428 (2018). doi:10.1016/bs.mcb.2017.08.023
18. Chalk, R. *et al.* High-Throughput Mass Spectrometry Applied to Structural Genomics. *Chromatography* **1**, 159–175 (2014).
19. Niesen, F. H., Berglund, H. & Vedadi, M. The use of differential scanning fluorimetry to detect ligand interactions that promote protein stability. *Nat. Protoc.* **2**, 2212–2221 (2007).
20. Chari, A. *et al.* ProteoPlex: Stability optimization of macromolecular complexes by sparse-matrix screening of chemical space. *Nat. Methods* **12**, 859–865 (2015).
21. Gorrec, F. The MORPHEUS protein crystallization screen. *J. Appl. Crystallogr.* **42**, 1035–1042 (2009).
22. Winter, G. Xia2: An expert system for macromolecular crystallography data reduction. *J. Appl. Crystallogr.* **43**, 186–190 (2010).
23. McCoy, A. J. *et al.* Phaser crystallographic software. *J. Appl. Crystallogr.* **40**, 658–674 (2007).
24. Afonine, P. V. *et al.* Towards automated crystallographic structure refinement with phenix.refine. *Acta Crystallogr. Sect. D Biol. Crystallogr.* **68**, 352–367 (2012).

25. Emsley, P., Lohkamp, B., Scott, W. G. & Cowtan, K. Features and development of Coot. *Acta Crystallogr. Sect. D Biol. Crystallogr.* **66**, 486–501 (2010).
26. Krojer, T. *et al.* The XChemExplorer graphical workflow tool for routine or large-scale protein-ligand structure determination. *Acta Crystallogr. Sect. D Struct. Biol.* **73**, 267–278 (2017).
27. Wojdyr, M., Keegan, R., Winter, G. & Ashton, A. DIMPLE - a pipeline for the rapid generation of difference maps from protein crystals with putatively bound ligands . *Acta Crystallogr. Sect. A Found. Crystallogr.* **69**, s299–s299 (2013).
28. Pearce, N. M. *et al.* A multi-crystal method for extracting obscured crystallographic states from conventionally uninterpretable electron density. *Nat. Commun.* **8**, 24–29 (2017).
29. Murshudov, G. N. *et al.* REFMAC5 for the refinement of macromolecular crystal structures. *Acta Crystallogr. Sect. D Biol. Crystallogr.* **67**, 355–367 (2011).